Journal of Biomolecular NMR, **21:** 249–261, 2001.
KLUWER/ESCOM

Amide proton temperature coefficients as hydrogen bond indicators in proteins

Tomasz Cierpicki & Jacek Otlewski*
Laboratory of Protein Engineering, Institute of Biochemistry and Molecular Biology, University of Wrocław, Poland

Received 27 August 2001; Accepted 28 August 2001

Key words: amide proton temperature coefficients, chemical shifts, hydrogen bonds, ring current, secondary structures

Abstract

Correlations between amide proton temperature coefficients ($\Delta\sigma_{HN}/\Delta T$) and hydrogen bonds were investigated for a data set of 793 amides derived from 14 proteins. For amide protons showing temperature gradients more positive than −4.6 ppb/K there is a hydrogen bond predictivity value exceeding 85%. It increases to over 93% for amides within the range between −4 and −1 ppb/K. Detailed analysis shows an inverse proportionality between amide proton temperature coefficients and hydrogen bond lengths. Furthermore, for hydrogen bonds of similar bond lengths, values of temperature gradients in α-helices are on average 1 ppb/K more negative than in β-sheets. In consequence, a number of amide protons in α-helices involved in hydrogen bonds shorter than 2 Å show $\Delta\sigma_{HN}/\Delta T < -4.6$ ppb/K. Due to longer hydrogen bonds, 90% of amides in 3_{10} helices and 98% in β-turns have temperature coefficients more positive than –4.6ppb/K. Ring current effect also significantly influences temperature coefficients of amide protons. In seven out of eight cases non-hydrogen bonded amides strongly deshielded by neighboring aromatic rings show temperature coefficients more positive than −2 ppb/K. In general, amide proton temperature gradients do not change with pH unless they correspond to conformational changes. Three examples of pH dependent equilibrium showing hydrogen bond formation at higher pH were found. In conclusion, amide proton temperature coefficients offer an attractive and simple way to confirm existence of hydrogen bonds in NMR determined structures.

Introduction

Amide proton temperature coefficients are easily measured, but they are only seldom used during protein structure analysis. Several attempts were carried out to use temperature coefficients for prediction of hydrogen bonds and evaluation of solvent accessibilities of amide protons in peptides (Dyson et al., 1988a, b; Krebs et al., 1998). However, the temperature induced chemical shift changes may be related to a decrease of the population of structured state upon heating which is confirmed by the observation of many anomalous temperature coefficients (Andersen et al., 1997). It can be stated that amide proton temperature coefficients are poor indicators of intramolecular hydrogen bonds in peptides (Baxter and Williamson, 1997).

More promising application of temperature coefficients concerns systems which do not display conformational averaging. The stable tertiary fold of proteins appears to be an appropriate target for this purpose. Analysis of $^1H^N$ temperature coefficients of BPTI and lysozyme showed almost linear changes of chemical shifts up to about 15° below the denaturation temperature (Baxter and Williamson, 1997). This results from linear expansion of the protein molecule with increasing temperature (Tilton et al., 1992). In consequence, the average hydrogen bond length increases with the temperature and amide proton chemical shift changes. Chemical shift gradients differ significantly for hydrogen bonded and non-hydrogen bonded amides (An-

*To whom correspondence should be addressed. E-mail: otlewski@bf.uni.wroc.pl

dersen et al., 1997), and in contrast with amide exchange rates, are almost pH independent (Baxter and Williamson, 1997). Recent work of Baxter et al. showed that not all chemical shifts in proteins change linearly with the temperature (Baxter et al., 1998). Such nonlinear changes may be used to characterize low-free energy excited states of folded proteins.

The main aim of this work was to evaluate usefulness of temperature gradients of amide protons in location of hydrogen bonds. The correlation of $^1H^N$ temperature gradients with hydrogen bonds has been already discussed (Andersen et al., 1997; Baxter and Williamson, 1997), but the conclusions were not generalized. Amide proton temperature coefficients bear potentially useful information for improving the quality of NMR structures. They may be used to confirm hydrogen bonds identified using geometrical criteria. We have already tested such approach during the structure determination of 69-residue protein, LUTI (Cierpicki and Otlewski, 2000). Hydrogen bonds were identified in preliminary structures applying both geometrical and $\Delta\sigma_{HN}/\Delta T$ criteria and successfully included in further calculations.

Theory

There is a strong temperature dependence of amide proton chemical shifts with the temperature (Kopple et al., 1969; Ohnishi and Urry, 1969). The main reason of this effect is related to the hydrogen bond presence. Chemical shifts depend on the inverse third power of the distance between amide proton and hydrogen bond acceptor (Wagner et al., 1983). The magnitude of thermal motions increases with the temperature, and it results in lengthening of average hydrogen bond lengths (Tilton et al., 1992). This, in turn, leads to a decrease of the deshielding effect induced by an acceptor and, in consequence, at higher temperature amide proton becomes shifted downfield to a lesser extent. Almost all amide protons in proteins are involved in intramolecular or intermolecular (with water) hydrogen bonds (McDonald and Thornton, 1994). As intermolecular hydrogen bonds are generally weaker, their structural perturbations are more pronounced and, therefore, $^1H^N$ chemical shifts are more temperature dependent. Stronger intramolecular hydrogen bonds are less susceptible to deformation and such amides show smaller chemical shift changes with temperature. This temperature dependence of $^1H^N$ shifts in proteins is more complicated. This is not only affected by hydrogen bond acceptor, but also are influenced by surrounding C=O and C−N bonds (Asakura et al., 1995) as well as ring current of neighboring aromatic side chains (Merutka et al., 1995).

Results

Temperature gradients of amide protons

The analysis reported here was based on a data set consisting of 793 amide protons derived from 14 proteins. Values of amide proton temperature coefficients ranged from −17.5 to 6.7 ppb/K with typical values falling within the −11 to 1 ppb/K range (about 98% of all cases). Analysis of temperature coefficients in the data set allowed us to divide all amide protons into three classes:

- amides forming hydrogen bonds (labeled A and B),
- amides not forming hydrogen bonds (labeled N),
- amides not forming hydrogen bonds and strongly shielded by neighboring aromatic rings (labeled R).

Identification of hydrogen bonds in proteins in an unambiguous manner is not simple, and the choice of cut-off values is often arbitrary. They were, therefore, identified based on more (A) and less stringent (B) criteria (see Material and methods). Results of our analysis are summarized in Table 1.

Amides forming hydrogen bonds

Amide protons involved in intramolecular hydrogen bonds form the most abundant group comprising two thirds (66.5%) of all cases. Distribution of the values of $^1H^N$ temperature gradients is shown in Figure 1. About 80% of all hydrogen bonded amides occur in the range between −5 and 0 ppb/K and their average value is -3.2 ± 2.0 ppb/K.

Amides not forming hydrogen bonds

About one third of backbone amides within our data set are not involved in intramolecular hydrogen bonds. They are in most cases solvent exposed and form intermolecular hydrogen bonds with water molecules. As shown in Figure 1 (dashed line) their temperature coefficients are significantly decreased, compared to hydrogen bonded amides (solid line) with the mean value equal to -7.1 ± 2.5 ppb/K (-6.9 ± 2.8 ppb/K when the third group of $^1H^N$ protons shielded by

Table 1. Statistics of hydrogen bonded and non-hydrogen bonded amide protons in 14 proteins. The hydrogen bonds are classified according to more (A) and less (B) stringent criteria (see Materials and Methods). Non-hydrogen bonded amide protons are divided into two groups (labeled N and R). The less abundant group (R) comprises non-hydrogen bonded amides strongly deshielded by neighboring aromatic rings. N is a total number of amide protons with known temperature coefficients; N_{HB} and N_{non-HB} stand for hydrogen bonded and non-hydrogen bonded $^1H^N$, respectively; N_A, N_B, N_N, N_R, N_{A+B}, N_{N+R} are numbers of amide protons in each group. The last two columns show Protein Data Bank (PDB) codes of analyzed structures. (a) Residues 10–144 from the N-terminal domain of phosphoglycerate kinase (see Materials and methods); (b) sum and percentage of amides in a particular group

Protein	N	N_{HB}		N_{non-HB}		N_{A+B}	N_{N+R}	X-ray	NMR
		N_A	N_B	N_N	N_R				
AMCI-I	51	22	2	27	–	24	27	–	1ccv
BNBD-12	32	13	4	15	–	17	15	–	1bnb
BPTI	53	29	3	19	2	32	21	5pti	1pit
C-551	74	51	2	21	–	53	21	451c	2pac
CT-CBH I	33	18	2	12	1	20	13	–	2cbh
CMTI-I	26	15	–	10	1	15	11	1ppe	3cti
ω-CgTx	23	18	3	2	–	21	2	–	1omc
EETI-II	23	10	3	10	–	13	10	–	2let
eglin c	63	37	4	22	–	41	22	1cse	1egl
IL-8	55	34	2	17	2	36	19	3il8	2il8
LUTI	65	41	–	23	1	41	24	–	1dwm
lysozyme	120	83	1	36	–	84	36	3lzt	–
N-PGK[a]	128	94	8	25	1	102	26	1php	–
T1	47	25	3	18	–	28	19	–	1tih
Sum[b]	793	490	37	258	8	527	266		
		61.8%	4.7%	32.5%	1.0%	66.5%	33.5%		

aromatic rings is included). About 82% of all non-hydrogen bonded amides lie within the range between −11 and −5 ppb/K. These values are similar to that observed for random coil peptides (Merutka et al., 1995).

Amides not forming hydrogen bonds but adjacent to aromatic rings

Amides belonging to the third group are much less abundant. They do not form hydrogen bonds and their chemical shifts are significantly upfield shifted due to the presence of neighboring aromatic rings. We found eight such examples in our data set and listed them in Table 5. The proximity of aromatic rings strongly influences both chemical shifts and their temperature gradients, lying typically between −2 and 0 ppb/K.

Hydrogen bonds versus temperature gradients

Our analysis showed that values of $\Delta\sigma_{HN}/\Delta T$ differ significantly for hydrogen bonded and non-hydrogen bonded $^1H^N$ protons (Figure 1). Therefore, we decided to calculate predictivity of the hydrogen bond presence as a function of amide temperature gradients. The values of $\Delta\sigma_{HN}/\Delta T$ were divided into 0.5 ppb/K ranges and the percentage of hydrogen bonded protons was calculated for each group (Figure 2). We concluded that hydrogen bond predictivity higher than 85% correspond to amide protons with temperature coefficients more positive than −4.6 ppb/K. Two observed extremes (−9 ppb/K and near 0.5 ppb/K) result probably from a small number of cases occurring at the border of typically observed values. It should be noticed that the elimination of amides adjacent to aromatic rings improves the correlation. The highest probability of the hydrogen bond presence, over 93%, is observed for amides with $\Delta\sigma_{HN}/\Delta T$ values ranging from −4 to −1 ppb/K. Such amides should be considered as very probable hydrogen bond donors. On the other hand, it should be stressed that a low value of the temperature gradient does not eliminate the presence of a hydrogen bond. A number of $^1H^N$ protons lying within the range between −7 and −5 ppb/K may

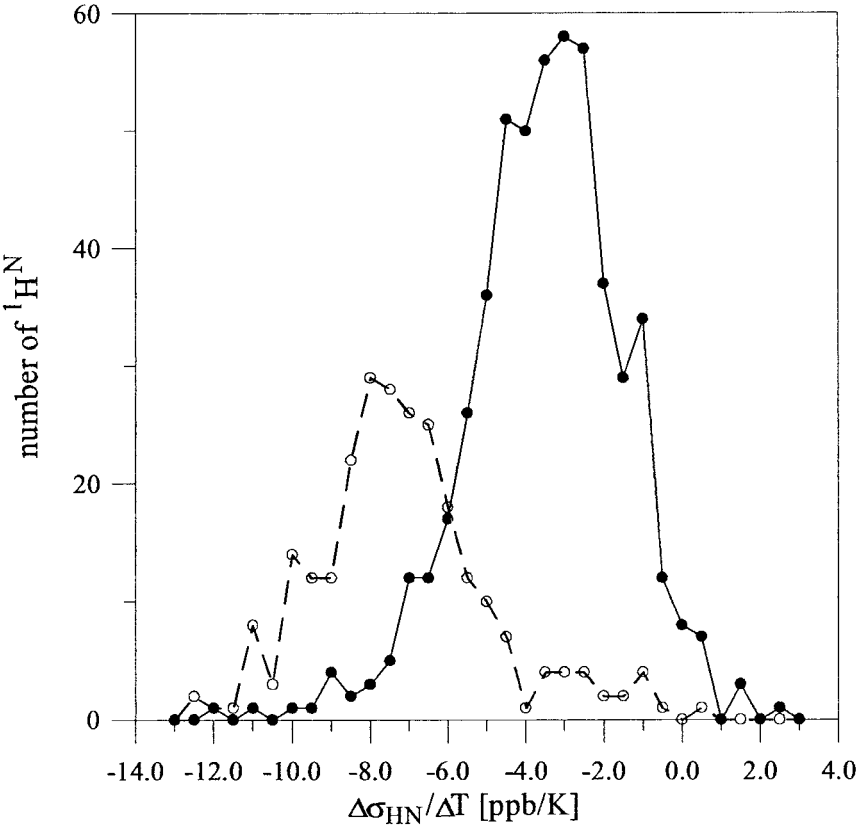

Figure 1. Plot of the distribution of $\Delta\sigma_{HN}/\Delta T$ values for $^1H^N$ protons in 14 proteins. For clarity, only the range between −13 and 3 ppb/K is shown, and non-hydrogen bonded amides strongly shielded by adjacent aromatic rings are not included. The solid line represents hydrogen bonded amides and the dashed line represents non-hydrogen bonded protons. The mean values of $\Delta\sigma_{HN}/\Delta T$ for the two groups are −3.2±2.0 ppb/K and −7.1±2.5 ppb/K, respectively.

form hydrogen bonds (Figure 2). This group includes a significant number of amides residing in α-helices (see below). Considering low negative temperature coefficients, it should be noted that in our database a hydrogen bond probability lower than 20% is observed for amides with $\Delta\sigma_{HN}/\Delta T$ more negative than −7 ppb/K.

The analysis of amide protons with temperature coefficients more positive than −4.6 ppb/K for each protein is shown in Table 2. The number of hydrogen bonded amides expressing $\Delta\sigma_{HN}/\Delta T \geq -4.6$ ppb/K was calculated. Typically, over 85% of the amide protons with temperature gradients more positive than −4.6 ppb/K were hydrogen bonded. The worst agreement was observed for BNBD-12 (76.2%) and T1 (78.6%). However, the poor correlations obtained for the two proteins may be due to imperfectly defined structures. In the case of BNBD-12, three non-hydrogen bonded amide protons with $\Delta\sigma_{HN}/\Delta T \geq -4.6$ ppb/K are located in poorly defined regions (RMSD for backbone atoms > 1.5 Å). Furthermore, N-terminal residues in T1 are not well defined, and four amide protons (residues 5, 6, 7 and 8) have $\Delta\sigma_{HN}/\Delta T \geq -4.6$ ppb/K but are not hydrogen bonded.

Amide proton temperature coefficients in secondary structures

The majority of hydrogen bonded backbone amide protons are found in secondary structures. Furthermore, such hydrogen bonds are accurately determined in lower quality structures. Thus, more detailed analysis was carried out for amides in one of four types of structures: α-helix, β-sheet, 3_{10}-helix or β-turn. As shown above, if the temperature coefficient is more positive than −4.6 ppb/K, there is a high probability that the amide is hydrogen bonded. The percentage of hydrogen bonded amides with temperature gradients more positive than −4.6 ppb/K was calculated for a

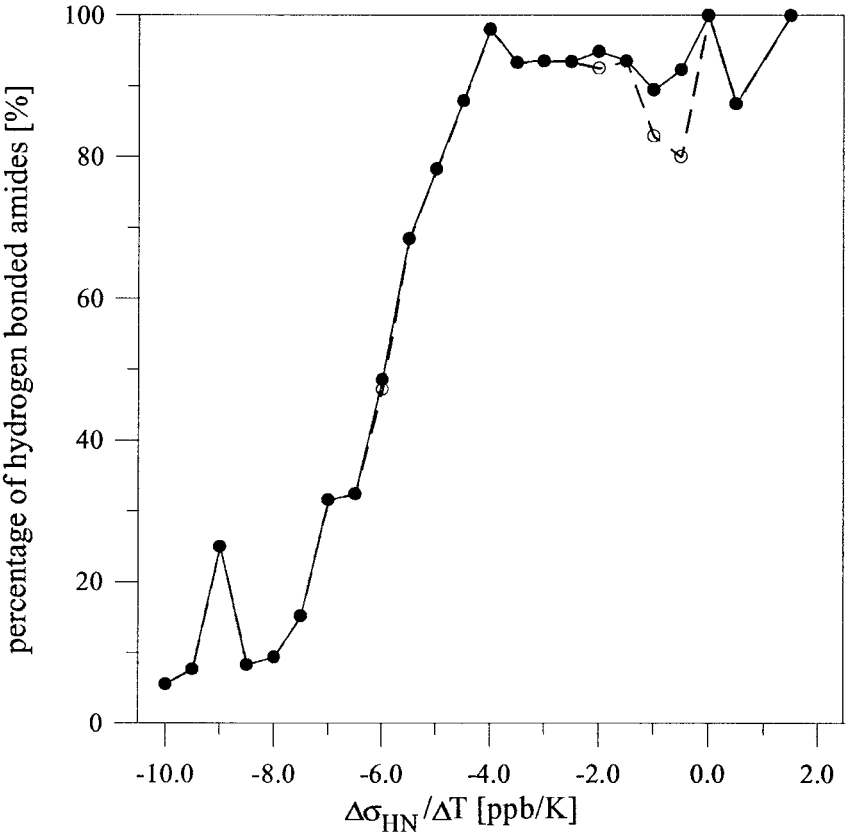

Figure 2. Hydrogen bond presence as a function of amide temperature gradients obtained for 14 proteins. Values of $\Delta\sigma_{HN}/\Delta T$ ranging from -10 to 2 ppb/K were grouped into 0.5 ppb/K ranges and the percentage of hydrogen amides for each group was calculated. Dashed line denotes relationship obtained for all amides and solid line was calculated after excluding non-hydrogen bonded $^1H^N$ protons shielded by aromatic rings.

particular secondary structure type (Table 3). The obtained values were different and the lowest percentage of hydrogen bonded amide protons with temperature coefficients more positive than -4.6 ppb/K was observed for α-helices (∼70%). Thus, a fraction of hydrogen bonded amides in α-helices with $\Delta\sigma_{HN}/\Delta T \geq -4.6$ ppb/K is even lower compared to values obtained for individual proteins (Table 2). For β-sheets and 3_{10}-helices, about 87 to 90% of amides fulfill the condition $\Delta\sigma_{HN}/\Delta T \geq -4.6$ ppb/K, while the excellent agreement, about 98% of amides with $\Delta\sigma_{HN}/\Delta T \geq -4.6$ ppb/K, was found for β-turns. This observation shows that occurrence of the hydrogen bond between $^1H^N$ of i-th residue and C=O of residue i-3 is very well correlated, with a small temperature gradient of the amide proton.

Influence of hydrogen bond distance on $\Delta\sigma_{HN}/\Delta T$

Availability of high resolution protein crystal structures allowed us to analyze relationship between $^1H^N$ temperature gradients and hydrogen bond lengths. Since protein side chains may exhibit conformational variability between solution and crystal, the analysis was carried out only for amide protons occurring in secondary structures. In order to obtain accurate distances, proteins with good quality crystal structures (resolution better than 2 Å) were considered. Measured $^1H^N$... O distances were stepped by 0.1 Å and for each distance range an average temperature coefficient and standard deviation were calculated (Figure 3). There is an obvious influence of the hydrogen bond length on the $^1H^N$ temperature coefficient. In general, large temperature gradients are observed for shorter hydrogen bonds while small temperature gradients exist for longer hydrogen bonds. For example, the average value of $\Delta\sigma_{HN}/\Delta T$ for short ($^1H^N$... O distances smaller than 1.8Å) and long ($^1H^N$... O distances longer than 2.3 Å) hydrogen bonds in α-helices is equal to -6.0 ± 0.5 and -2.3 ± 1.9 ppb/K, respectively. This tendency originates from the inverse

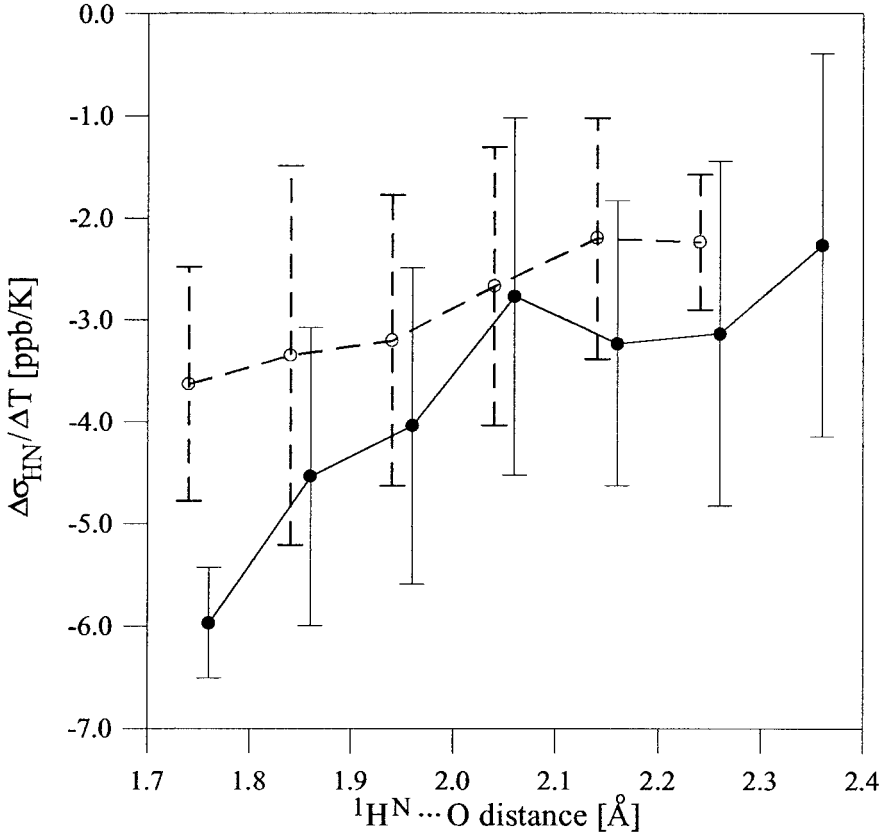

Figure 3. Dependence of the $^1H^N$ temperature coefficient on hydrogen bond length. Solid and dashed lines represent values for α-helices and β-sheets, respectively. All $^1H^N$... O distances were grouped to 0.1 Å ranges for which the average $\Delta\sigma_{HN}/\Delta T$ values were calculated. Vertical lines stand for standard deviations. The two amides, $^1H^N$ Val99 ($\Delta\sigma_{HN}/\Delta T = -8.1$ ppb/K) and $^1H^N$ Ser100 ($\Delta\sigma_{HN}/\Delta T = 3.6$ ppb/K) from helix 3 in lysozyme were excluded from the analysis. Their anomalous temperature gradients show lack of correlation between $\Delta\sigma_{HN}$ and hydrogen bond length (Figure 6). This may results from either a differences between crystal and solution or local conformational changes upon warming.

third power dependence of amide chemical shifts on hydrogen bond length (Wagner et al., 1983). The temperature-induced increase in hydrogen bond length results in less deshielding of amide proton. Due to the cubic dependence of the effect, a similar amplitude of thermal motion causes different chemical shift changes for short and long hydrogen bonds. Therefore, larger $^1H^N$ temperature gradients are expected for shorter hydrogen bonds (Contreras et al., 1997).

Distribution of hydrogen bond lengths varies between different secondary structures (Figure 4). The shortest hydrogen bonds dominate in β-sheets while longer hydrogen bonds are typical for 3_{10}-helices and β-turns. Due to helix curvature, numerous short, as well as long hydrogen bonds are observed in α-helices. The distribution shows that in 3_{10}-helices and β-turns hydrogen bonds usually exceed 2 Å. Owing to the dependence of the temperature gradients on hydrogen bond lengths for distances longer than 2 Å, their values are usually more positive than −4.6 ppb/K, regardless of the secondary structure type (Figure 3). In consequence, over 90% of amides in 3_{10}-helices and 98% in β-turns exhibit $\Delta\sigma_{HN}/\Delta T$ values more positive than −4.6 ppb/K (Table 3).

Hydrogen bonds in α-helices and β-sheets

About 87% of hydrogen bonded amides in β-sheets exhibit $\Delta\sigma_{HN}/\Delta T$ more positive than −4.6 ppb/K, while the correlation is 70% in α-helices (Table 3). In general, more negative temperature gradients were observed for shorter hydrogen bonds, both in α-helices and β-sheets (Figure 3). However, the values of temperature coefficients are on average 1 ppb/K lower for α-helices than for β-sheets. For example, mean values of $\Delta\sigma_{HN}/\Delta T$ for hydrogen bond length range between 1.8 and 1.9 Å are equal to -3.3 ± 1.9 and

Table 2. Statistics for amide protons with temperature coefficients more positive than −4.6 ppb/K. $N_{-4.6}$ stands for the total number of $^1H^N$ protons with $\Delta\sigma_{HN}/\Delta T \geq -4.6$ ppb/K; $N_{-4.6,HB}$ is the number of hydrogen bonded $^1H^N$ protons, with $\Delta\sigma_{HN}/\Delta T \geq -4.6$ ppb/K (percentages are shown in parentheses)

Protein	$N_{-4.6}$	$N_{-4.6,HB}$ (%)
AMCI-I	20	20 (100)
BNBD-12	21	16 (76.2)
BPTI	30	28 (93.3)
C-551	38	33 (86.8)
CT-CBH I	21	19 (90.5)
CMTI-I	12	11 (91.7)
ω-CgTx	17	17 (100)
EETI-II	10	10 (100)
eglin c	33	31 (93.9)
IL-8	37	33 (89.2)
LUTI	40	36 (90.0)
lysozyme	63	59 (93.7)
N-PGK	92	87 (94.6)
T1	28	22 (78.6)

Table 3. Hydrogen bonded amide protons with temperature coefficients more positive than −4.6 ppb/K found in four types of secondary structure. N_{HB} indicates the total number of hydrogen bonded $^1H^N$ protons in a particular secondary structures; $N_{-4.6,HB}$ (%) stands for the number and percentage of hydrogen bonded $^1H^N$ protons with $\Delta\sigma_{HN}/\Delta T \geq -4.6$ ppb/K

Secondary structure	N_{HB}	$N_{-4.6,HB}$ (%)
α-helix	129	90 (69.8)
β-sheet	122	106 (86.9)
3_{10}-helix	41	37 (90.2)
β-turn	49	48 (98.0)

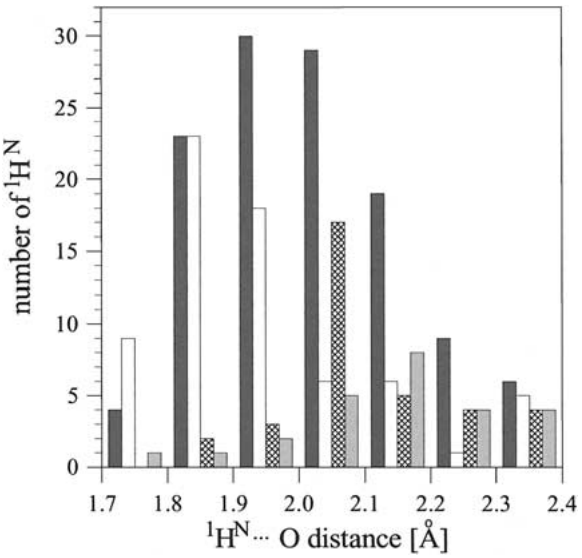

Figure 4. Distribution of hydrogen bond lengths within four types of secondary structures: α-helix (dark gray bars), β-sheet (white bars), 3_{10}-helix (dashed bars), β-turn (light gray bars). Hydrogen bond lengths were stepped by 0.1 Å.

Table 4. Amide protons in AMCI-I, BPTI and lysozyme with pH dependent temperature coefficients, $\Delta(\Delta\sigma_{HN}/\Delta T) \geq 1.5$ ppb/K. The values of amide proton temperature coefficients [pbb/K] determined at lower and higher pH are in the second and third columns, respectively. Since $\Delta\sigma_{HN}/\Delta T$ of Glu49 at low pH was not reported previously we measured it at pH = 2.9

	Lower pH	Higher pH	Hydrogen bond acceptor
AMCI-I	pH=2.5	pH=4.6	
Gly4	−4.1	−2.4	Glu7 OE
Thr25	−11.0	−9.1	–
Arg44	−5.9	−9.0	–
Gly46	−5.3	−3.4	–
BPTI	pH=2.9	pH=4.6	
Glu49	−5.2	−3.7	Glu49 OE
lysozyme	pH=3.8	pH=5.0	
Cys30	−3.6	−1.4	Gly26 O
Thr89	−5.7	−3.4	Asp87 OD
Gly102	−8.5	−6.8	Val99 O

−4.5±1.5 ppb/K for β-sheets and α-helices, respectively. Furthermore, the difference becomes more pronounced for shorter hydrogen bonds.

In contrast to $\Delta\sigma_{HN}/\Delta T$, the chemical shift deviation, $\Delta\sigma_{HN}$, is inversely proportional to hydrogen bond length (Wagner et al., 1983). The detailed analysis of chemical shifts of hydrogen bonded amide protons allowed us to find a difference between conformational shifts, $\Delta\sigma_{HN}$, in α-helices and β-sheets. It is well known that $^1H^N$ protons of residues in β-sheet regions experience downfield shifts, whereas those in α-helix regions experience upfield shifts in comparison to the random coil values. This difference is usually related to different average hydrogen bond lengths within the two types of secondary structures (Wishart et al., 1991). However, our analysis showed that even for identical hydrogen bond lengths the values of $\Delta\sigma_{HN}$ are on average 0.4 ppm larger in α-

helices than in β-sheets (Figure 5). Thus, this effect is not only related to the distance between amide proton and hydrogen bonded carbonyl oxygen. The difference between amide proton chemical shifts in regular secondary structures was explained based on empirical calculations (Asakura et al., 1995). Downfield shift of amide protons in β-sheets is caused predominantly by hydrogen bonded carbonyl oxygen. However, hydrogen bonded $^1H^N$ (residue i) in α-helix is not only influenced by neighboring C=O (residue i−4) but also by C=O (residue i−3) and C−N (residue i−2) bond anisotropies (Asakura et al., 1995). In consequence, the peptide bond anisotropies of neighboring residues contribute significantly to the shielding of amide protons and cancel the deshielding effect caused by the hydrogen bonded carbonyl. Therefore, compared to random coil values, amide chemical shifts are downfield and upfield shifted in β-sheets and α-helices, respectively.

In our opinion the same mechanism is responsible for the difference in temperature gradients of amide protons between α-helices and β-sheets. Adjacent peptide bonds which influence the amide chemical shifts in α-helices also affect their temperature dependence.

Temperature shifts of amide protons in α-helices

The asymmetric distribution of polar and nonpolar residues and packing effects frequently result in curvature of protein and peptide α-helical structures. This leads to variation of hydrogen bond lengths between the two sides of helices and 3–4 residue oscillations of $\Delta\sigma_{HN}$ values (Kuntz et al., 1991; Zhou et al., 1992). A significant correlation between $\Delta\sigma_{HN}$ and $^1H^N$ temperature coefficients was noticed for helical peptides (Contreras et al., 1997). The effect was also related to helix curvature as amide proton temperature gradients varied between both helix sides.

The correlation of conformational shifts ($\Delta\sigma_{HN}$), hydrogen bond lengths and temperature gradients was analyzed for amide protons in 14 α-helices within our protein data set. The plots showing correlation of hydrogen bond distances, conformational shifts ($\Delta\sigma_{HN}$) and temperature coefficients against residue number are shown in Figure 6. As expected, the hydrogen bond length varies along the sequences of all 14 helices. In most cases a 3–4 residue periodic pattern is observed. Maxima of conformational chemical shifts ($\Delta\sigma_{HN}$) correspond to minima of hydrogen bond lengths. Simultaneously, the hydrogen bond lengths correlate with $^1H^N$ temperature gradients. Low negative values of $\Delta\sigma_{HN}/\Delta T$ correspond to shorter hydrogen bonds, as shown in Figure 3.

As mentioned above a number of hydrogen bonded amide protons in α-helices show temperature coefficients more negative than −4.6 ppb/K. These amides are usually located on the concave face of a curved helix and are involved in short hydrogen bonds. In most cases they exhibit positive values of $\Delta\sigma_{HN}$ (data not shown).

Effect of pH on $^1H^N$ temperature coefficients

Attempts to differentiate solvent exposed and buried amide protons were one of the first applications of $^1H^N$ temperature coefficients in proteins (Nielsen et al., 1994, 1995). However, amide proton temperature coefficients being almost pH independent are not appropriate indicators of exposition to solvent. The analysis carried out for three proteins, AMCI-I (Cierpicki et al., 2000), BPTI and lysozyme (Baxter and Williamson, 1997) revealed that differences in $\Delta\sigma_{HN}/\Delta T$ between lower (2.5–3.8) and higher (4.6–5.0) pH are very small.

We found eight amide protons with pH induced changes of temperature coefficients, ($\Delta\Delta\sigma_{HN}/\Delta T$) larger than 1.5 ppb/K (Table 4). Regardless of pH three temperature gradients were more negative than −5.9 ppb/K (Thr25 and Arg44 in AMCI-I; Gly102 in lysozyme) and two were more positive than −4.1 ppb/K (Gly4 in AMCI-I; Cys30 in lysozyme). However, for three amide protons (Gly46 in AMCI-I; Glu49 in BPTI; Thr89 in lysozyme) $\Delta\sigma_{HN}/\Delta T < -4.6$ ppb/K and $\Delta\sigma_{HN}/\Delta T > -4.6$ ppb/K were observed for lower and higher pH, respectively. The common feature of the three amides was close proximity of acidic side chains. Analysis of solution structure of AMCI-I (determined at pH 2.5) showed no hydrogen bonds with $^1H^N$ Gly46. However, the side chain of neighboring Glu47 may serve as potential hydrogen bond acceptor. In the x-ray structure of lysozyme, $^1H^N$ Thr89 forms a hydrogen bond with side chain of Asp87. Analysis of BPTI crystal structures, indicated that $^1H^N$ Glu49 may form hydrogen bond with its side chain carboxyl group (PDB code 5pti) or that this hydrogen bond may be absent in another structure (PDB code 1bhc). In all three cases variation of $\Delta\sigma_{HN}/\Delta T$ as a function of pH may indicates equilibrium between hydrogen bonded and non-hydrogen bonded states. Because a hydrogen bond with a negatively charged carboxyl group is stronger (Fersht, 1987), the equilibrium is moved

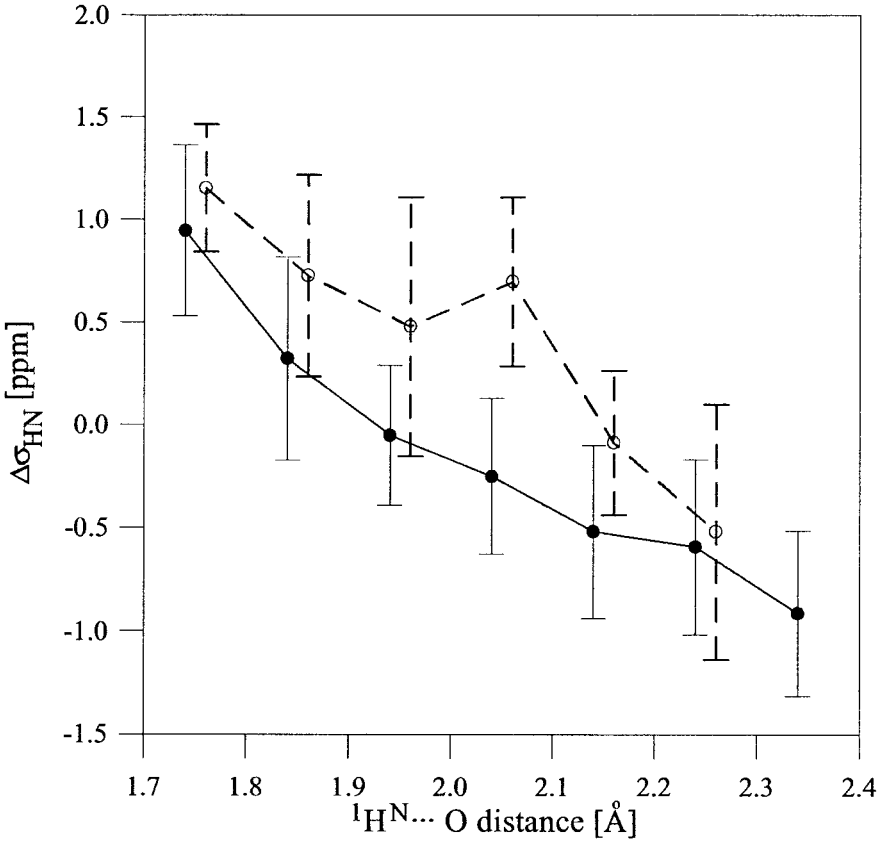

Figure 5. Dependence of $^1H^N$ chemical shift deviation ($\Delta\sigma_{HN}$) on hydrogen bond length. The solid line is for α-helices and the dashed line for β-sheets. All $^1H^N$... O distances were grouped to 0.1 Å ranges for which average $\Delta\sigma_{HN}$ values were calculated. Vertical lines stand for standard deviations. Conformational shifts of amide protons, $\Delta\sigma_{HN}$, correspond to the difference between measured and random coil chemical shifts at 25 °C.

into hydrogen bond formation at higher pH ($\Delta\sigma_{HN}/\Delta T > -4$ ppb/K). An increase in population of non-hydrogen bonded state for protonated acid side chains at lower pH ($\Delta\sigma_{HN}/\Delta T < -5$ ppb/K) is observed. Analysis of amide proton temperature gradients may be used to follow such pH induced structural changes.

Influence of aromatic ring on $^1H^N$ temperature changes

As mentioned above, the ring current effect strongly influences amide proton temperature shifts. We examined all amides deshielded by at least 1 ppm, relative to random coil values. Of the total 50 deshielded amides, eight were affected by neighboring aromatic rings and not hydrogen bonded. The upfield shifted amides for which no potential acceptor atom was found within 3 Å radius are shown in Table 5. All $^1H^N$ temperature gradients, except one example, are significantly more positive than −4.6 ppb/K. This effect can be explained by a strong influence of the ring current on $^1H^N$ chemical shifts. In consequence, the increase of thermal motions does not cause meaningful chemical shift changes. An unusually large positive $\Delta\sigma_{HN}/\Delta T$ value (6.7 ppb/K) was observed in case of $^1H^N$ Gly15 of CT-CBH I. Such an effect may be related to the temperature-induced conformational change and increase of an average distance between amide proton and aromatic ring. This leads to weaker deshielding of $^1H^N$ Gly15 and positive chemical shift change. In another case, the amide proton of Gly12 in BPTI is affected by the neighboring aromatic ring of Tyr10 and shows $\Delta\sigma_{HN}/\Delta T$ equal to −5.9 ppb/K. Larger temperature gradient of $^1H^N$ could be related to configurational changes of solvent exposed side chain of Tyr10 due to temperature raise. In conclusion, it is worthwhile to emphasize that an adjacent aromatic ring can significantly affect both amide chemical shift and its temperature coefficient.

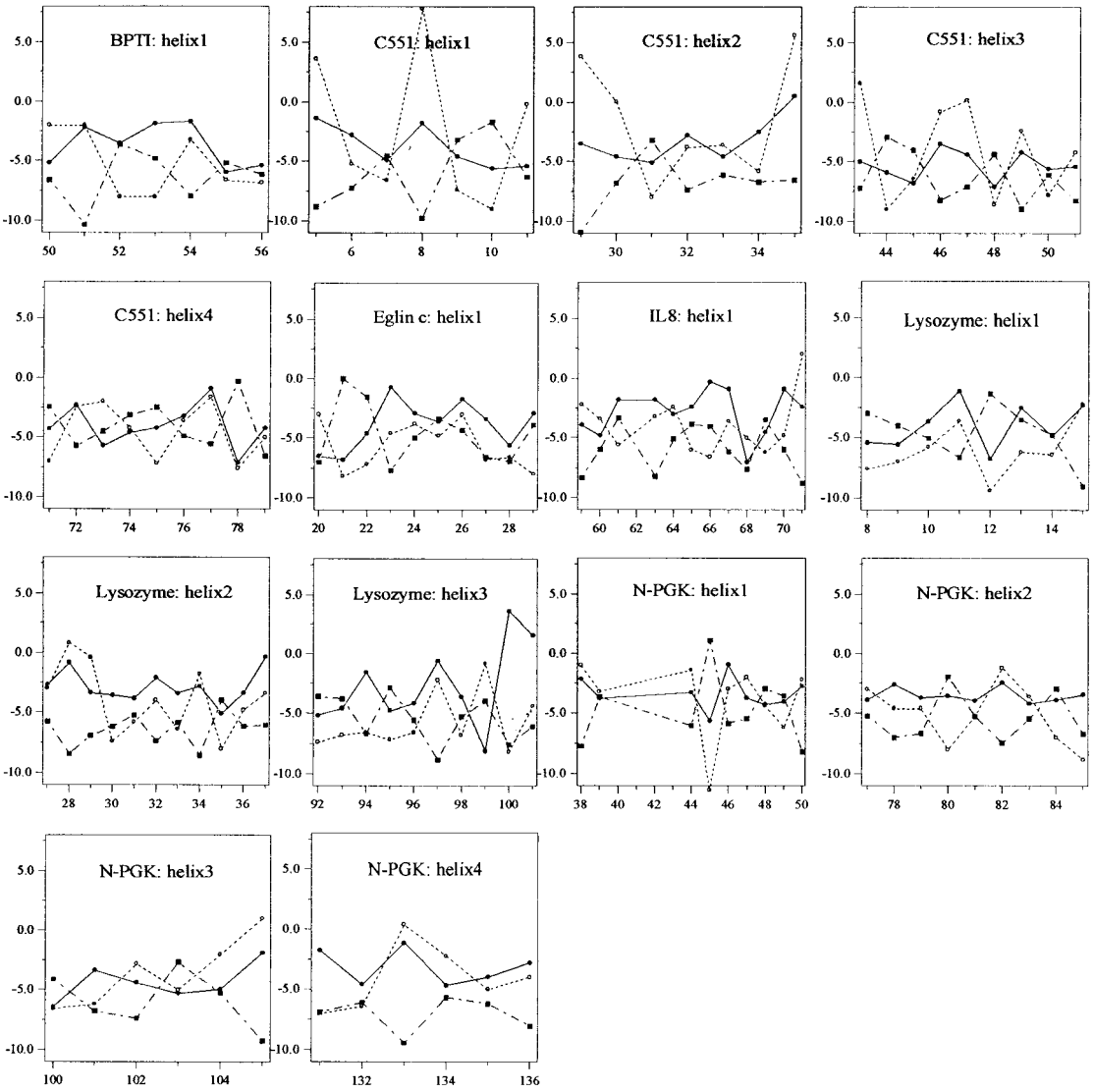

Figure 6. Correlation of hydrogen bond length (....○....), conformational shift, $\Delta\sigma_{HN}$ (●—● ■ ●—●) and amide proton temperature coefficient (—●—) against residue number in 14 α-helices. Vertical scale represents $\Delta\sigma_{HN}/\Delta T$ [ppb/K]. The values of $^1H^N$... O distances ($d_{HN...O}$) [Å] and $\Delta\delta_{HN}$ [ppm] were scaled to fit to the plots using the following formulas: $20^*d_{HN...O} - 45$ and $4^*\Delta\delta_{HN} - 5$.

Amide protons that are strongly deshielded by aromatic rings (the temperature gradients within the range between −2 and 0 ppb/K) may indicate weak hydrogen bonds (Desiraju and Steiner, 1999). The arrangement of amide protons with respect to aromatic rings is not random (Mitchell et al., 1994) and could provide favorable interactions since the π-electron cloud may act as hydrogen bond acceptor (Levitt and Perutz, 1988). This interaction may be half as strong as a normal hydrogen bond and it could have an effect on the orientation of aromatic side chains in folded protein structures (Cheney et al., 1988). Analysis performed by Mitchell et al., 1994) showed that within the database of 55 non-homologous protein chains, 67 main-chain amides were in 'above ring' contacts. Such interactions may occur between neighboring residues (short range) as well as between sequentially distant residues (long range). An example of short range contacts is represented by a frequently studied interaction in BPTI between amide proton of Gly37 (one of the most shielded amide proton in diamagnetic proteins) and the aromatic side chain of Tyr35 (Cheney et al., 1988). A long range case was found in N-PGK between $^1H^N$ Val68 and the aromatic ring of Phe119.

Table 5. Amide protons found in data set of 14 proteins that are not involved in intramolecular hydrogen bonds but are strongly deshielded by neighboring aromatic rings

Protein	$^1H^N$	σ_{HN} (ppm)	$\Delta\delta_{HN}$ (ppm)	$\Delta\sigma_{HN}/\Delta T$ (ppb/K)	Neighboring aromatic sidechain
BPTI	Gly12	7.18	−1.10	−5.9	Tyr10
BPTI	Gly37	4.32	−3.96	0.0	Tyr35
CT-CBH I	Gly15	5.16	−3.12	6.7	Tyr13
CMTI-I	Tyr27	6.87	−1.24	−1.9	Tyr27
IL8	Lys15	6.29	−1.90	−0.9	Tyr13
IL8	Phe17	5.86	−2.39	−0.3	Phe17
LUTI	Ala9	6.67	−1.54	−1.0	Trp10
N-PGK	Val68	5.47	−2.61	−0.7	Phe119

In conclusion, the amide proton temperature gradients are a valuable source of information and can be used to confirm hydrogen bonds during protein structure refinement. In general, amide proton temperature coefficients more positive than −4.6 ppb/K indicate hydrogen bonds. However, we showed that it can occur in some cases for amides not involved in hydrogen bond as the result of deshielding effects caused by aromatic rings, by pH dependent hydrogen bond formation, or may be present in poorly defined regions. Additionally, we feel that the collection of larger data set of $\Delta\sigma_{HN}/\Delta T$ values would further expand application of amide proton temperature coefficients in identification of hydrogen bonds in proteins.

Materials and methods

Collection of protein $^1H^N$ database

The data base of amide proton temperature coefficients was collected from data reported in the literature. Additionally, we supplemented it with data obtained for three proteins investigated in our laboratory (AMCI-I, CMTI-I, LUTI). Altogether, the chemical shifts and temperature gradients of amide protons were analyzed for 14 proteins: *Apis mellifera* chymotrypsin/cathepsin G inhibitor I (AMCI-I) (Cierpicki et al., 2000), bovine neutrophil β-defensin-12 (BNBD-12) (Zimmermann et al., 1995), bovine pancreatic trypsin inhibitor (BPTI) (Baxter and Williamson, 1997), C-terminal domain comprising residues 462-497 of cellobiohydrolase I (CT-CBH I) (Kraulis et al., 1989), *Cucurbita maxima* trypsin inhibitor I (CMTI-I) (this work), ω-conotoxin GVIA (ω-CgTx) (Davis et al., 1993), ferrocytochrome C-551 from *Pseudomonas aeruginosa* (C-551) (Timkovich, 1990), *Ecballium elaterium* trypsin inhibitor II (EETI-II) (Nielsen et al., 1994), eglin c (Heinz et al., 1992), interleukin 8 (IL-8) (Rajarathnam et al., 1996), *Linum usitatissimum* trypsin inhibitor (LUTI) (Cierpicki and Otlewski, 2000), hen egg-white lysozyme (Baxter and Williamson, 1997), N-terminal domain of *B. stearothermophilus* phosphoglycerate kinase (N-PGK) (Baxter et al., 1998), trypsin inhibitor from *Nicotiana alata* (T1) (Nielsen et al., 1995). Altogether, the data contained 793 points providing the largest data base of protein amide proton temperature coefficients.

Amide proton temperature coefficients were measured for isolated N-terminal domain (residues 1–174) of 45 kDa 3-phosphoglycerate kinase (PGK) (Baxter et al., 1998). However, only crystal structure of intact enzyme is known (PDB code 1php). Previous NMR study showed that isolated N-terminal domain is almost unaffected compared to the whole protein (Hosszu et al., 1997). The only difference was found in region perturbed by loss of C-terminal domain (residues 148–152). In our analysis we used only amide protons for residues 10-144 which are distant from residues contacting C-terminal domain.

Determination of hydrogen bonds

Amide protons forming hydrogen bonds were identified from three-dimensional protein structures (Table 1). In cases, when NMR and X-ray derived structures were available, we used both of them. Protons were added to X-ray determined structures using standard geometrical criteria available in MOLMOL program (Koradi et al., 1996). The program was also

used for identification of hydrogen bonds. All amides were classified into one of four groups:

A – hydrogen bonded – acceptor atom found within the distance of 2.5 Å from amide proton, angle between the line from the backbone nitrogen atom and amide proton and line from the backbone nitrogen atom and acceptor atom smaller than 40 degrees;

B – hydrogen bonded – acceptor atom found within the distance smaller than 3.0 Å and the angle between the line from the backbone nitrogen atom and amide proton and line from the backbone nitrogen atom and acceptor atom smaller than 50 or 60 degrees for X-ray and NMR determined structures, respectively;

N – non-hydrogen bonded;

R – non-hydrogen bonded, but strongly shielded by aromatic ring (more than 1 ppm).

In case of NMR structures hydrogen bond was accepted only if it was present in at least 50% of all conformers. All hydrogen bonded amides were arranged in two categories (A and B). Application of less stringent criterion (B) was used in order to find weaker hydrogen bonds and to consider possible errors in protein structure determination.

NMR spectroscopy

CMTI-I was isolated from figleaf gourd (*Cucurbita ficifolia*) (Otlewski et al., 1984). Amide proton temperature coefficients were determined for CMTI-I. ^{1}H NMR spectra were recorded on a Bruker DRX 300MHz spectrometer at temperatures 300, 308, 315 and 325 K. Protein sample was dissolved in H_2O/D_2O (10:1) mixture to a concentration of 5 mM. The pH value was adjusted to 4.5 adding small amounts of NaOH. A set of TOCSY spectra were recorded using standard pulse sequence (Braunschweiler and Ernst, 1983). Water signal was supressed by presaturation. Spectra were processed and analysed in NMRPipe (Delaglio et al., 1995) and Sparky (Goddard and Kneller) programs, respectively. Amide proton chemical shifts were determined on the basis of previously published assignments (Nilges et al., 1991). Temperature coefficients of $^1H^N$ protons were calculated as best fits to experimental data points. Conformational shifts of amide protons, $\Delta\sigma_{HN}$, correspond to the difference between measured and random coil chemical shifts at 25 °C (Andersen et al., 1997).

Acknowledgements

We thank Dr Michael P. Williamson for amide proton temperature coefficients for N-PGK. This project was supported by grant 6PO4A 02119 from the Polish Committee for Scientific Research.

References

Andersen, N.H., Neidigh, J.W., Harris, S.M., Lee, G.M., Liu, Z. and Tong, H. (1997) *J. Am. Chem. Soc.*, **119**, 8547–8561.

Asakura, T., Taoka, K., Demura, M. and Williamson, M.P. (1995) *J. Biomol. NMR*, **6,** 227–236.

Baxter, N.J. and Williamson, M.P. (1997) *J. Biomol. NMR*, **9**, 359–369.

Baxter, N.J., Hosszu, L.L., Waltho, J.P. and Williamson, M.P. (1998) *J. Mol. Biol.*, **284**, 1625–1639.

Braunschweiler, L. and Ernst, R.R. (1983) *J. Magn. Reson.*, **53**, 521–528.

Cheney, J., Cheney, B.V. and Richards, W.G. (1988) *Biochim. Biophys. Acta.*, **954**, 137–139.

Cierpicki, T. and Otlewski, J. (2000) *J. Mol. Biol.*, **302**, 1179–1192.

Cierpicki, T., Bania, J. and Otlewski, J. (2000) *Protein Sci.*, **9**, 976–984.

Contreras, M.A., Haack, T., Royo, M., Giralt, E. and Pons, M. (1997) *Lett. Pept. Sci.*, **4**, 29–39.

Davis, J.H., Bradley, E.K., Miljanich, G.P., Nadasdi, L., Ramachandran, J. and Basus, V.J. (1993) *Biochemistry*, **32**, 7396–7405.

Delaglio, F., Grzesiek, S., Vuister, G.W., Zhu, G., Pfeifer, J. and Bax, A. (1995) *J. Biomol. NMR*, **6**, 277–293.

Desiraju, G. and Steiner, T. (1999). *The Weak Hydrogen Bond in Structural Chemistry and Biology*, Oxford University Press, Oxford.

Dyson, H.J., Rance, M., Houghten, R.A., Lerner, R.A. and Wright, P.E. (1988a) *J. Mol. Biol.*, **201**, 161–200.

Dyson, H.J., Rance, M., Houghten, R.A., Wright, P.E. and Lerner, R.A. (1988b) *J. Mol. Biol.*, **201**, 201–17.

Fersht, A.R. (1987) *TIBS* **12**, 301–304.

Goddard, T.D. and Kneller, D.G. *SPARKY 3*, University of California, San Francisco.

Heinz, D.W., Hyberts, S.G., Peng, J.W., Priestle, J.P., Wagner, G. and Grutter, M.G. (1992) *Biochemistry*, **31**, 8755–8766.

Hosszu, L.L., Craven, C.J., Spencer, J., Parker, M.J., Clarke, A.R., Kelly, M. and Waltho, J.P. (1997) *Biochemistry*, **36**, 333–340.

Kopple, D.K., Ohnishi, M. and Go, A. (1969) *J. Am. Chem. Soc.*, **91**, 4264–4272.

Koradi, R., Billeter, M. and Wüthrich, K. (1996) *J. Mol. Graph.*, **14**, 51–55.

Kraulis, J., Clore, G.M., Nilges, M., Jones, T.A., Pettersson, G., Knowles, J. and Gronenborn, A.M. (1989) *Biochemistry*, **28**, 7241–7257.

Krebs, D., Maroun, R.G., Sourgen, F., Troalen, F., Davoust, D. and Fermandjian, S. (1998) *Eur. J. Biochem.*, **253**, 236–44.

Kuntz, I.D., Kosen, P.A. and Craig, E.C. (1991) *J. Am. Chem. Soc.*, **113**, 1406–1408.

Levitt, M. and Perutz, M.F. (1988) *J. Mol. Biol.*, **201**, 751–754.

McDonald, I.K. and Thornton, J.M. (1994) *J. Mol. Biol.*, **238**, 777–793.

Merutka, G., Dyson, H.J. and Wright, P.E. (1995) *J. Biomol. NMR*, **5**, 14–24.

Mitchell, J.B., Nandi, C.L., McDonald, I.K., Thornton, J.M. and Price, S.L. (1994) *J. Mol. Biol.*, **239**, 315–331.
Nielsen, K.J., Alewood, D., Andrews, J., Kent, S.B. and Craik, D.J. (1994) *Protein Sci.*, **3**, 291–302.
Nielsen, K.J., Heath, R.L., Anderson, M.A. and Craik, D.J. (1995) *Biochemistry*, **34**, 14304–14311.
Nilges, M., Habazettl, J., Brunger, A.T. and Holak, T.A. (1991) *J. Mol. Biol.*, **219**, 499–510.
Ohnishi, M. and Urry, D.W. (1969) *Biochem. Biophys. Res. Commun.*, **36**, 194–202.
Otlewski, J., Polanowski, A., Leluk, J. and Wilusz, T. (1984) *Acta Biochim. Pol.*, **31**, 267–278.
Rajarathnam, K., Clark-Lewis, I., Dewald, B., Baggiolini, M. and Sykes, B.D. (1996) *FEBS Lett.*, **399**, 43–46.
Tilton, R.F., Dewan, J.C. and Petsko, G.A. (1992) *Biochemistry*, **31**, 2469–2481.
Timkovich, R. (1990) *Biochemistry*, **29**, 7773–7780.
Wagner, G., Pardi, A. and Wuthrich, K. (1983) *J. Am. Chem. Soc.*, **1983**, 5948–5949.
Wishart, D.S., Sykes, B.D. and Richards, F.M. (1991) *J. Mol. Biol.*, **222**, 311–333.
Zhou, N.E., Zhu, B., Sykes, B.D. and Hodges, R.S. (1992) *J. Am. Chem. Soc.*, **114**, 4320–4326.
Zimmermann, G.R., Legault, P., Selsted, M.E. and Pardi, A. (1995) *Biochemistry*, **34**, 13663–13671.